Anal. Chem. **2007,** *79,* 2556−2561

Fabrication of Boron-Doped Diamond Ultramicroelectrodes for Use in Scanning Electrochemical Microscopy Experiments

Katherine B. Holt,*,† Jingping Hu,‡ and John S. Foord‡

Department of Chemistry, University College London, 20 Gordon Street, London WC1H 0AJ, United Kingdom, and Chemistry Research Laboratory, University of Oxford, Mansfield Road, Oxford OX1 3TA, United Kingdom

Boron-doped diamond (BDD) ultramicroelectrode (UME) tips were fabricated by the growth of BDD films by chemical vapor deposition onto sharpened tungsten wires. Both nanocrystalline and microcrystalline forms of diamond coatings were examined. The diamond-coated wires were selectively insulated with nail varnish, electrophoretic paint, or fast-setting epoxy to form UME tips of critical dimensions of 1−25 μm. The geometry of the exposed electrode area was disk or hemispherical in most cases. Cyclic voltammetry and chronoamperometry were used to assess exposed electrode area and integrity of the insulation. BDD UMEs were used to obtain SECM approach curves to an insulating and a conducting substrate, which were fitted to the theory appropriate for the observed tip geometry. The tips were used to obtain SECM images of immobilized respiring *E. coli*, illustrating the suitability of BDD UMEs for electrochemical imaging in biological media.

This paper introduces the use of boron-doped diamond (BDD) UME tips in SECM experiments. BDD is an electrode material that has attracted increasing attention due to its wide potential window in aqueous solution, low background currents, and lack of surface electrochemistry such as oxide formation or dissolution.[1] When highly doped, BDD couples metallic conductivity with desirable intrinsic material properties of diamond; it is robust, hard, and inert. BDD exhibits an impressive resistance to fouling and electrode deactivation in comparison to other electrode materials.[2] BDD is deposited as a thin layer on a substrate using chemical vapor deposition (CVD), and growth conditions can be tailored to produce polycrystalline diamond films of different thickness, crystal size, roughness, dopant level (conductivity), and graphitic sp^2 content.

SECM is a scanning probe technique, which uses an ultramicroelectrode (UME) tip to approach closely to the substrate under study and probe its electrochemical activity. In the feedback mode of SECM, the potential of the tip is selected to oxidize or reduce at steady state a redox mediator in solution. In bulk solution, this will result in a constant tip current of a magnitude defined by the electrode dimensions and geometry and the mediator concentration and diffusion coefficient. As the tip is moved toward the substrate from bulk solution, there is a characteristic decrease in current as the tip approaches an insulator (negative feedback) and an increase in current as the tip approaches a conductor (positive feedback). The plot of the tip current versus distance is known as an approach curve, and the experimental data can be fit to theoretical simulated curves that take into account the UME geometry and dimensions. Theoretical treatment has been developed for disk,[3] conical,[4] hemispherical,[5] spherical,[6] and ring[7] geometries of UMEs. An UME is defined as an electrode with one dimension less than 25 μm, and the insulation surrounding the electrode is usually very thin so that the ratio of the radius of the insulation to the radius of the disk (the RG) is as small as possible.

BDD microelectrodes have previously been fabricated by several research groups. Cooper[8] used microwave plasma CVD to deposit diamond onto electrochemically etched tungsten wires that were then sealed in glass and the electrode exposed by polishing or etching in HF. Inlaid disk electrodes of radius 2−7 μm were produced. Fujishima has employed band-like diamond microelectrodes in an end column electrochemical detector for capillary electrophoresis.[9] Martin et al.[10] deposited BDD diamond films onto a 25 μm diameter W wire presealed in a quartz glass tube, resulting in electrodes of diameter 30 μm with unusual grain structure due to different diamond growth rates on the quartz and the W. Recently, a nanodiamond microprobe electrode has

* To whom correspondence should be addressed. E-mail: k.b.holt@ucl.ac.uk.
† University College London.
‡ University of Oxford.

(1) For a review, see: Compton, R. G.; Foord, J. S.; Marken, F. *Electroanalysis* **2003**, *15*, 1349.
(2) (a) Muna, G. W.; Tasheva, N.; Swain, G. M. *Environ. Sci. Technol.* **2004**, *38*, 3674. (b) Shin, D.; Fujishima, A.; Merkoci, A.; Wang, J. *Chem. Sens.* **2003**, *19B*, 130. (c) Sarada, B. V.; Rao, T. N.; Tryk, D. A.; Fujishima, A. *New Diamond Front. Carbon Technol.* **1999**, *9*, 365. (d) Xu, J.; Chen, Q.; Swain, G. M. *Anal. Chem.* **1998**, *70*, 3146. (e) Saterlay, A. J.; Foord, J. S.; Compton, R. G. *Electroanalysis* **2001**, *13*, 1065.
(3) Bard, A. J.; Fan, F. R. F.; Kwak, J.; Lev, O. *Anal. Chem.* **1989**, *61*, 132.
(4) Zoski, C. G.; Liu, B.; Bard, A. J. *Anal. Chem.* **2004**, *76*, 3646.
(5) Sezler, Y.; Mandler, D. *Anal. Chem.* **2000**, *72*, 2383.
(6) Demaillle, C.; Brust, M.; Tsionsky, M.; Bard, A. J. *Anal. Chem.* **1997**, *69*, 2323.
(7) Lee, Y.; Amemiya, S.; Bard, A. J. *Anal. Chem.* **2001**, *73*, 2261.
(8) Cooper, J. B.; Pang, S.; Albin, S.; Zheng, J.; Johnson, R. B. *Anal. Chem.* **1998**, *70*, 464.
(9) Shin, D.; Sarada, B. V.; Tryk, D. A.; Fujishima, A. *Anal. Chem.* **2003**, *75*, 530.
(10) Xie, S.; Shafer, G.; Wilson, C. G.; Martin, H. B. *Diamond Relat. Mater.* **2006**, *15*, 225.

10.1021/ac061995s CCC: $37.00
Published on Web 02/13/2007

been produced by insulating a diamond-coated wire with photoresist and exposing the electrode tip by lithography giving a conical tip with radius of about 50 μm.[11] Swain has produced diamond microelectrodes for use in capillary electrophoresis[12] and in biological environments.[13] The use of different insulation methods was explored, resulting in electrodes of mixed cylindrical/conical geometry of diameter ~70 μm, although smaller electrodes were mentioned.

Despite activity in this field, there is no previous report of the reproducible fabrication of UMEs less than 25 μm of well-defined geometry that would be suitable for use in SECM experiments.

EXPERIMENTAL METHODS

(i) Growth of CVD Boron-Doped Diamond Tips on Sharpened W Wires. Tungsten wire (Goodfellow Ltd., Cambridge, UK) was electrochemically etched in 2 M NaOH using a DC voltage to obtain a sharpened tip.[14] To avoid the blunting of the tip after the wire cleaves in the etching solution, a controller circuit with cut off time of 500 ns was incorporated into the power supply, and sharp tips with diameter less than 100 nm were routinely achieved. The sharpened wire was ultrasonically seeded in a ~3.5 nm nanodiamond powder (Yorkshire Bio Ltd.) suspension for 30 min.

The seeded W tips were positioned 5 mm below the filament in the Hot Filament CVD chamber. The microcrystalline diamond thin film coatings were deposited from 0.3% to 0.7% CH_4 in H_2 source gas (BOC), which was bubbled through trimethylborate (Sigma-Aldrich Ltd., 99%) before entering the reaction chamber. The tungsten tips were heated at 800−1000 °C by direct heating from the filament; the total gas flow was 165 sccm, the chamber pressure was 33 mbar, and the deposition time was usually 10 h. To obtain nanodiamond, higher methane concentrations of 3% were used, and a negative electrical bias was applied to the tungsten tips.[15]

(ii) Insulation Methods. BDD-coated W wires were fixed at the uncoated end to a copper wire with silver conducting paint (Electrolube, RS Components) to form a contact. The wire was placed in a glass capillary tube to add rigidity and allow mounting in the SECM instrument. For nail varnish (NV) insulation, the whole assembly was coated, and the very tip of the BDD coated wire was exposed to form an UME by gently touching it to filter paper that was barely wetted with acetone. Alternatively, fast setting epoxy (FE) was prepared and sucked into one end of a glass capillary tube. The BDD-coated wire was threaded into the tube from the opposite end, sharpened tip first, until the tip was level with the opening of the tube and completely coated with epoxy. The epoxy was then left to cure overnight at room temperature. The hardened epoxy was gently polished with wet and dry paper and 0.05 μm alumina to expose the tip of the BDD electrode.

The use of electrophoretic paint (EP) to insulate sharpened Pt wires and produce very small SECM tips exploits the fact that these paint coatings tend to shrink back from sharp surface features.[16] For the cathodic paints used in this work, the BDD electrode was used as the cathode, a platinum coil was used as the anode, and a potential of 5 V was applied for 30 s. The paint-coated electrode was cured in an oven at 180 °C for 30 min. However, the shrinking method only worked occasionally for our diamond electrodes. Completely insulated electrodes were therefore purposefully fabricated, using more severe electrodeposition conditions of DC voltage of 20 V for 3 min, and then exposing the tip end by abrading on fine mesh wet and dry paper.

(iii) Electrochemistry and SECM. Electrochemical experiments were carried out with an Autolab PSTAT10 bipotentiostat (EcoChemie, Netherlands), and approach curves were performed using a Burleigh piezo positioner with a P-100 controller. SECM imaging was carried out with a CHI 900 SECM (CH Instruments, Austin, TX).

Electrochemistry of the BDD-coated wires was tested before and after insulation using cyclic voltammetry (CV) of ferrocene methanol (FcOH), $Ru(NH_3)_6^{3+}$, and $IrCl_6^{2-}$. The effectiveness of the insulation was tested using chronoamperometry and monitoring how the steady-state current at the tip changed as it was moved from air into solution using the piezo positioner. An increase in limiting current as the electrode was further submerged in solution was indicative of pinholes in the insulation down the shaft of the electrode. SECM approach curves were carried out to a conductor (platinum electrode) and an insulator (flat PTFE insulation around the electrode) at an approach rate of 4.6 μm s^{-1}. *Escherichia coli* (ATCC # 25922) was obtained in pellets from TCS BioSciences (UK) and grown in LB Miller broth (Fisher Scientific) with D-glucose (Fisher Scientific), until the stationary phase. The cells were harvested by centrifugation and then immobilized onto a glass slide using poly-L-lysine (Sigma-Aldrich). The immobilized cells were used as a substrate for SECM imaging experiments, obtained by scanning in the $x-y$ plane at a scan rate of 300 μm s^{-1} using an electrode located 5 μm above the cells.

RESULTS AND DISCUSSION

(i) Electrode Characterization by SEM, Optical Microscopy, and Raman Spectroscopy. Diamond growth took place slowly on the smooth etched W tips, as indicated in Figure 1a, due to difficulties in nucleation, which tend to occur at areas of surface roughness.[17] Nucleation was promoted by ultrasonic treatment of the wire in a nanodiamond powder suspension, which roughened the surface and embedded nanodiamonds to act as nucleation centers. This resulted in uniform coverage of the etched tip, as can be seen in Figure 1b. Typical film thicknesses for these coatings were determined by SEM of fractured tips, illustrated in Figure 1c, and are of the order of 8 μm.

Alternative growth conditions were employed to increase nucleation and growth rate, leading to smoother coatings with

(11) Basu, S.; Kang, W. P.; Davidson, J. L.; Choi, B. K.; Bonds, A. B.; Cliffel, D. E. *Diamond Relat. Mater.* **2006**, *15*, 269.

(12) Cvacka, J.; Quaiserova, V.; Park, J.; Show, Y.; Muck, A.; Swain, G. M. *Anal. Chem.* **2003**, *75*, 2678.

(13) Park, J.; Show, Y.; Quaiserova, V.; Galligan, J. J.; Fink, G. D.; Swain, G. M. *J. Electroanal. Chem.* **2005**, *583*, 56.

(14) Ibe, J. P.; Bey, P. P.; Brandow, S. L.; Brizzolara, R. A.; Burnham, N. A.; Dilella, D. P.; Lee, K. P.; Marrian, C. R. K.; Colton, R. J. *J. Vac. Sci. Technol., A* **1990**, *8*, 3570.

(15) (a) Sharda, T.; Umeno, M.; Soga, T.; Jimbo, T. *Appl. Phys. Lett.* **2000**, *77*, 4304. (b) Jiang, N.; Sugimoto, K.; Nishimura, K.; Shintani, Y.; Hiraki, A. *J. Cryst. Growth* **2002**, *242*, 362.

(16) (a) Slevin, C. J.; Gray, N. J.; Macpherson, J. V.; Webb, M. A.; Unwin, P. R. *Electrochem. Commun.* **1999**, *1*, 282. (b) Zhu, L.; Claude-Montigny, B.; Gattrell, M. *Appl. Surf. Sci.* **2005**, *252*, 1833. (c) Chen, S. L.; Kucernak, A. *Electrochem. Commun.* **2002**, *4*, 80.

(17) Liu, Y. K.; Tso, P. L.; Lin, I. N.; Tzeng, Y.; Chen, Y. C. *Diamond Relat. Mater.* **2006**, *15*, 234.

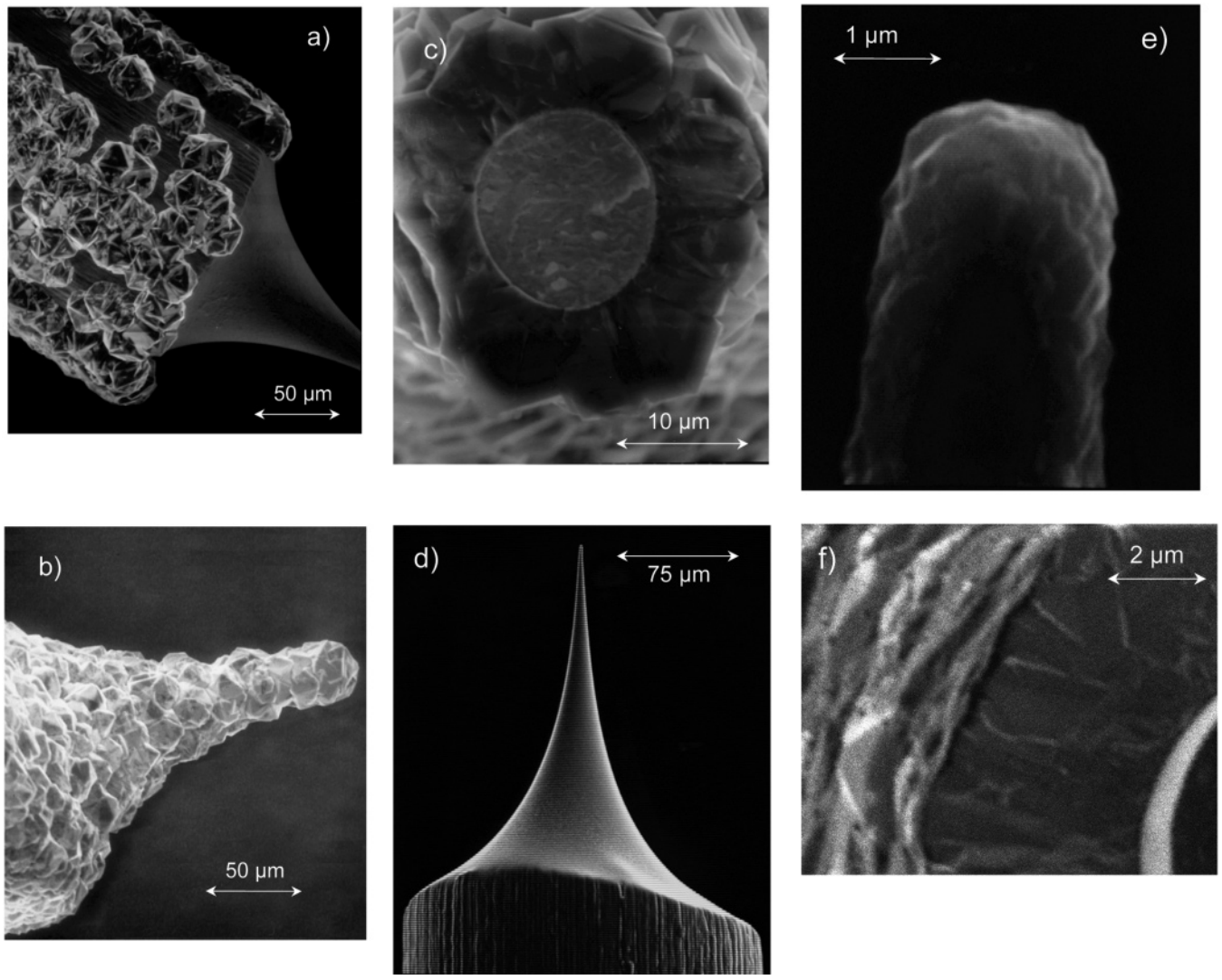

Figure 1. SEM images of (a) CVD BDD growth on sharpened tungsten wire without prior seeding, 12 h growth; (b) microcrystalline BDD growth on nanodiamond seeded W wire, 10 h growth; (c) cross section of broken tip; (d) smooth nanocrystalline diamond film grown by negative bias-enhanced growth; (e) sharp electrode tip achieved by bias-enhanced growth of nanocrystalline diamond; and (f) cross section through broken tip coated with electrophoretic paint.

smaller crystallites. Methane concentration was increased to around 3%, and a negative electrical bias was applied to the tungsten substrate for bias-enhanced growth. This results in good conformality, as shown in the SEM images in Figure 1d and e, and a grain size in the submicrometer range.

Raman spectra were taken of the two types of coatings. The microcrystalline diamond films exhibited only one strong peak: the diamond mode at 1332 cm^{-1}. The diamond films grown under electrical bias at higher methane concentrations show Raman spectra characteristic of small grain, nanocrystalline diamond.[18] A peak observed at 1130 cm^{-1} is associated with non-diamond polyacetylene-type structures in the grain boundaries, whereas broad peaks around 1350 and 1500 cm^{-1} are associated with disordered sp^2 carbon.

After insulation, the electrodes were examined using SEM or optical microscopy to determine exposed tip dimensions. For NV-insulated electrodes, the geometry of the exposed electrode was disk or hemispherical depending on the sharpness of the BDD-coated wire. The thickness of the NV insulation was estimated to be about 1 μm, giving a small RG between 1 and 2. The insulating layer of the EP-coated electrodes was very thin, only about 0.1 μm, when less extreme coating conditions (5 V for 30 s) were employed, as shown in Figure 1f. For microcrystalline films, retraction of the paint from the tip on curing was rarely observed, but sharp edges of the diamond crystallites could be observed, suggesting pinholes in the coating. The smoother nanocrystalline films resulted in better paint coverage, and more vigorous coating conditions resulted in coatings that were several micrometers thick. FE sealed electrodes are robust to polishing and of a better defined geometry; however, it was found that occasionally air bubbles form in the epoxy, resulting in a recessed or lagooned diamond electrode.

(ii) Electrochemical Characterization by Cyclic Voltammetry. The BDD electrodes were characterized by CV prior to insulation, as shown in Figure 2a. For the microcrystalline BDD

(18) Prawer, S.; Nemanich, R. J. *Philos. Trans. R. Soc. London, Ser. A* **2004**, *362*, 2537.

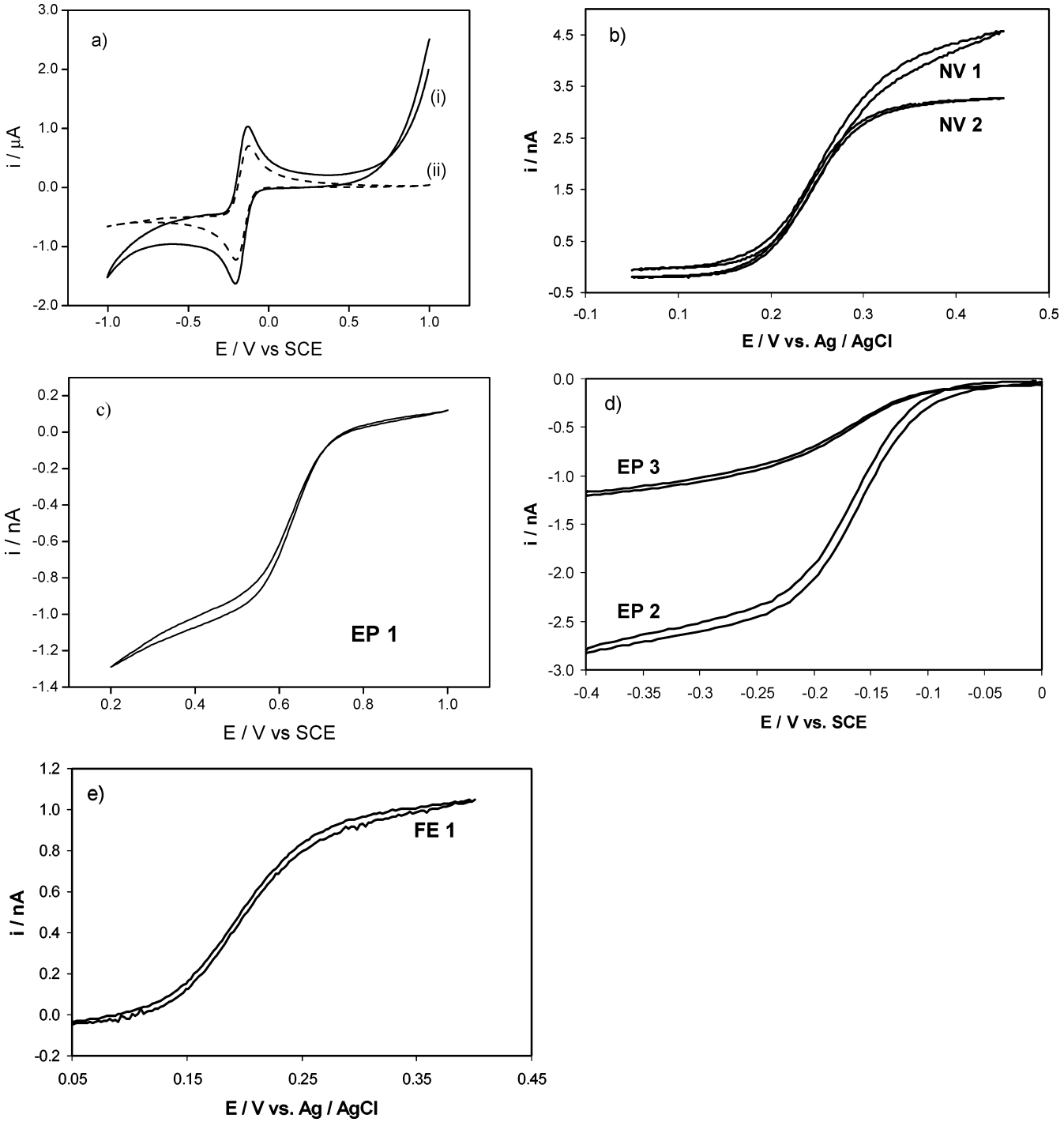

Figure 2. Cyclic voltammograms of (a) BDD electrodes before insulation, in 1 mM $Ru(NH_3)_6^{3+}$ in 0.1 M KCl, (i) nanocrystalline diamond, (ii) microcrystalline diamond; (b) UMEs obtained by insulation with nail varnish (NV 1 and NV 2), 1 mM FcOH in 0.1 M KCl, 10 mV s^{-1}; (c) UME obtained by shrinkage of electrophoretic paint (EP 1), 1 mM $IrCl_6^{2-}$ in 0.1 M KCl, 10 mV s^{-1}; (d) UMEs obtained by insulating with electrophoretic paint and exposing tip by polishing (EP 2 and EP 3), 1 mM $Ru(NH_3)_6^{3+}$ in 0.1 M KCl, 10 mV s^{-1}; and (e) UME obtained by insulation in fast setting epoxy (FE 1), 1 mM FcOH in 0.1 M KCl, 10 mV s^{-1}.

electrodes, reversible voltammetry for $Ru(NH_3)_6^{3+}$ is observed. No additional features, typical of cracks in the BDD coating and leakage to the underlying W, are observed. The potential window is reduced for the nanodiamond BDD, so some hydrogen and oxygen evolution is visible in the CV.

Figure 2b shows CVs obtained for NV-insulated electrodes, showing the sigmoidal shape associated with fast mass transfer and steady-state behavior. Under the microscope, NV 1 was of disk geometry, and $i_{lim} = 4.5$ nA is consistent with an electrode radius of 11 μm if an RG of 1.1 is assumed.[19] NV 2 was of hemispherical geometry, and $i_{lim} = 3.3$ nA suggests a hemispherical electrode of 7 μm radius. The Tomes criterion $|E_{3/4} - E_{1/4}|$ for these CVs is 56 mV, the predicted value for reversible electron-transfer kinetics.

(19) Shoup, D.; Szabo, A. *J. Electroanal. Chem.* **1984**, *160*, 27.

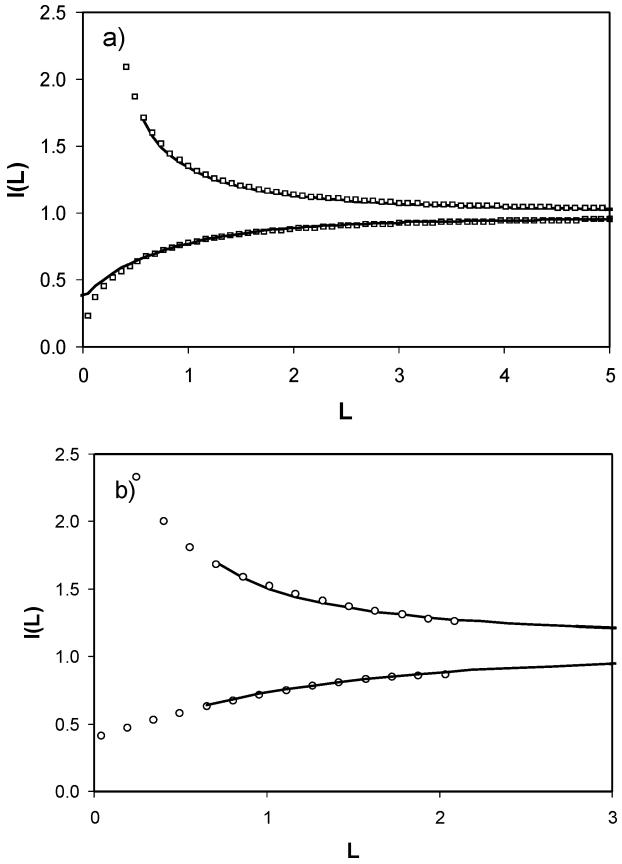

Figure 3. Experimental approach curves (black lines) to an insulator (PTFE) and a conductor (Pt electrode at 0 V) in 1 mM FcOH at an approach rate of 4.6 μm s^{-1} and tip potential 0.4 V along with appropriate theoretical curves (□): (a) For electrode NV 1, theoretical approach curves for a disk geometry tip with radius 11.5 μm and RG = 1.1; (b) for electrode NV 2, theoretical approach curves for a hemispherical geometry tip with radius 6 μm.

In a few cases, EP was found to retract from the tip to produce an UME; an example is shown in Figure 2c, of tip EP 1, showing $i_{lim} = 1.1$ nA in 1 mM $IrCl_6^{2-}$, corresponding to a tip radius of ~3 μm (assuming RG = 1.1 and a disk geometry). Gentle polishing of the paint-insulated tips also produced UMEs as shown in Figure 2d: EP 2 ($i_{lim} = 2.7$ nA) and EP 3 ($i_{lim} = 1.25$ nA) correspond to $a = 7$ μm and $a = 3.25$ μm, respectively (assuming disk geometry and RG = 1.1). Insulation in FE also resulted in very small electrodes as in Figure 2e, where $i_{lim} = 1.05$ nA corresponds to a 3.5 μm radius disk electrode (FE 1) with RG of 10.

(iii) Approach Curves to an Insulator and a Conductor. Electrodes NV 1 and NV 2 were used to obtain approach curves to an insulator and a conductor. NV 1 is believed to be of disk geometry, radius 11 μm, and RG of 1.1 from CV measurements and microscopy. The experimental approach curves for this electrode are shown in Figure 3a along with the theoretical curves predicted for a disk electrode.[20] The experimental data fit well to theory over the range $L = 5$ to $L = 0.5$ assuming a disk radius of 11.5 μm and an RG of 1.1. This is consistent with microscopy observations and CV measurements. Electrode NV 2 is assumed to be of hemispherical geometry and of radius 6−7 μm from optical and CV measurements. This was confirmed by the experimental approach curves shown in Figure 3b, which showed an excellent fit to theory for negative and positive feedback of a hemispherical electrode,[12] assuming a radius of 6 μm. Both experimental approach curves showed the tip making contact with the substrate at a separation of about 5 μm even though the RG was very small in both cases, which is a normal result for the home-built experimental setup used in these experiments, where substrate tilt and vibration cannot be effectively eliminated. The experimental curves in Figure 3a suggest that closer approach is possible to an insulator than a conductor; however, close inspection shows the experimental curve begins to deviate from the theoretical one at approximately the same distance. The current continues to fall for the negative feedback curve because the PTFE insulator is relatively soft, and deformation by the harder BDD allows further tip movement toward the surface.

(iv) SECM Imaging of the RC Function of *E. coli*. To demonstrate the suitability of BDD UME tips for SECM applications, they were used for imaging the respiratory activity of immobilized *E. coli*. Bacteria were fixed to a glass slide using poly-L-lysine and treated with 10 mM ferricyanide, 0.05 M pH 7 PBS, 0.1 M $NaNO_3$, and 0.05 M glucose. As the *E. coli* respire, ferricyanide is reduced by respiratory chain (RC) enzymes, with the resulting formation of ferrocyanide.[9] A microscope image of the immobilized *E. coli* is shown in Figure 4a. BDD UME tip EP 1, formed by shrinkage of EP, was used to detect ferrocyanide produced by the respiring cells and hence obtain an image of the immobilized bacteria. This electrode was used as it had a small tip radius of about 3 μm (Figure 2c) and a small RG. The tip was located approximately 5 μm above the cells by performing a negative feedback approach curve to the glass slide. The potential of the tip was 0 V vs Ag/AgCl to detect ferrocyanide produced by the cells.

Under these conditions, it has been found that *E. coli* can produce ferrocyanide at a rate of 10^{-17} mol s^{-1} $cell^{-1}$ as they respire.[21] The maximum concentration of ferrocyanide at 5 μm height above the cells is expected to be in the order of 1×10^{-5} M, leading to maximum tip currents in the order of 10 pA. It is therefore necessary to use an UME tip that has a very low background current and is extremely sensitive to low concentrations of redox mediator as well as being fairly small and sharp so that it can approach closely to the cells. In addition, the solution contains high concentrations of glucose and other biomolecules produced by the living cells; hence, the electrode must show resistance to fouling. BDD is an excellent electrode material for this application, as shown by the SECM image shown in Figure 4b. To the left of the image, zero current is observed as the tip passes over the glass slide, but as it moves over the *E. coli*, the tip currents increase due to production of ferrocyanide by the bacteria. The currents over the cells vary from 3 to 12 pA, as predicted, depending on the density of the immobilized cells. This illustrates that even the nanodiamond electrode used to record this image has low enough background currents and is sensitive enough to detect such small currents. It is anticipated that the microcrystalline BDD would perform even better. Experiments are currently underway to systematically compare the performance of Pt UMEs and BDD UMEs in this application, where it is expected that BDD will be more reliable in this fouling media.

(20) *Scanning Electrochemical Microscopy*; Bard, A. J., Mirkin, M. V., Eds.; Marcel Dekker: New York, 2001; p 156.

(21) Holt, K. B. Unpublished data.

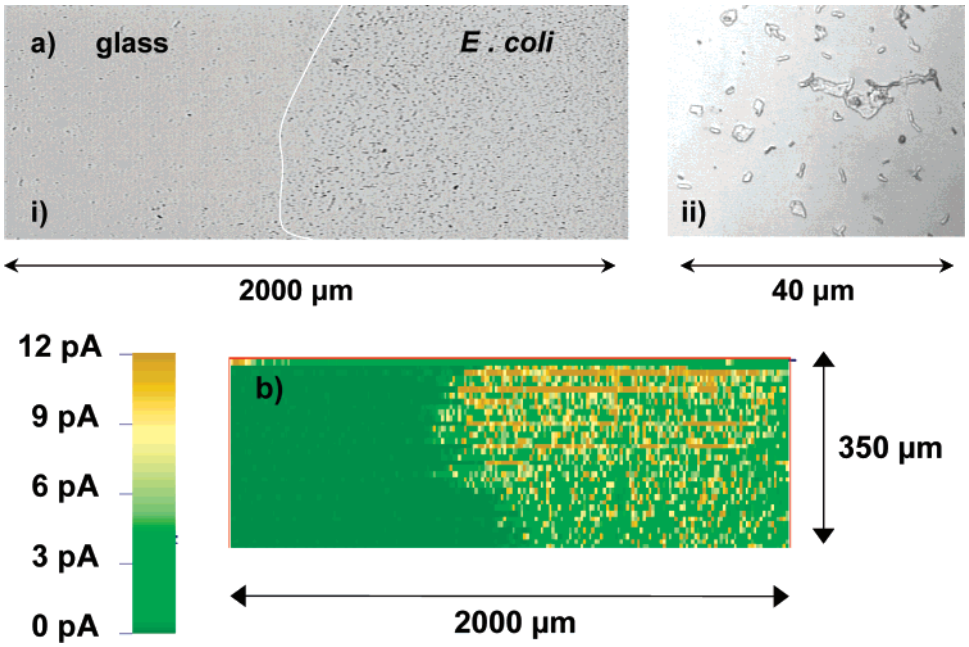

Figure 4. (a) Optical microscope images using (i) ×5 objective, of *E. coli* immobilized onto a glass slide using poly-L-lysine (cells are immobilized on the right-hand side of the slide as demarked by a white line); (ii) ×50 objective, immobilized *E. coli* showing isolated cells of about 2 μm in length as well as aggregated clumps of cells. (b) SECM image of immobilized *E. coli* cells obtained by detecting ferrocyanide produced by the cells as they respire (see text). Obtained using BDD UME tip EP 1 of radius ~3 μm, rastered in the $x-y$ plane at 300 μm s^{-1} approximately 5 μm above the cells with tip potential 0 V vs Ag/AgCl.

CONCLUSION

BDD UMEs of <25 μm and a range of geometries have been fabricated and used to obtain approach curves and image electrochemical activity of *E. coli* cells. Two types of BDD coating were developed: microcrystalline diamond with highly faceted and rough morphology, and a smooth nanocrystalline diamond. The latter has better morphology, especially for coating with thin insulation, such as electrophoretic paint. However, the former has a broader potential window for imaging at extreme potentials and lower background currents but requires thicker insulation methods, for example, nail polish or epoxy. For this reason, we are currently exploring different growth procedures for the formation of microcrystalline-type diamond but with smaller (1 μm) crystal sizes, and hence smoother films, to fully exploit the excellent properties of BDD UMEs in SECM experiments.

ACKNOWLEDGMENT

K.B.H. acknowledges the Ramsay Trust and Kodak for a Ramsay Fellowship, Dr. Daren J. Caruana, University College London, for use of equipment, and Dr. Darren A. Walsh, University of Newcastle-Upon-Tyne, for use of the CHI 900 SECM. This work was funded by EPSRC grant no. EP/D504813/1. J.H. is thankful for the generous financial support of the Newton Abraham studentship.

Received for review October 24, 2006. Accepted January 12, 2007.

AC061995S